Indian Journal of Chemistry
Vol. 55A, June 2016, pp. 686-691

One-step synthesis of ZnO nanowires on zinc foils and their photocatalytic properties

Mohamad Mohsen Momeni*

Department of Chemistry, Isfahan University of Technology, Isfahan 84156-83111, Iran
Email: mm.momeni@cc.iut.ac.ir

Received 01 June 2015; revised and accepted 23 May 2016

ZnO nanostructures with different morphologies have been grown on zinc foil substrate by a novel and facile hydrothermal method, without the assistance of any catalyst or template. The obtained ZnO samples are characterized by SEM, EDX, XRD, UV-visible and photoluminescence techniques. The resulting ZnO nanorod has a diameter of about 70-90 nm and the average length is estimated to be in the range of 0.5-2.0 μm. It is shown that the as-grown ZnO samples have a very good crystallinity. A comparison of the photocatalytic degradation of methyl orange with different ZnO shows that the photocatalytic properties of the ZnO nanostructures depend on the morphology of ZnO. The growth process of the ZnO nanorods is proposed based on the solid-liquid-solid mechanism.

Keywords: Oxides, Zinc oxide, Nanostructures, Nanorods, Morphology, Hydrothermal synthesis, Photocatalytic activity.

Properties of nanomaterials depend on various characteristics such as crystal structures, morphologies and chemical compositions[1]. Direct preparation of nanostructures with controllable orientation, density and crystalline morphology is important in the field of nanoscience. Among various semiconductors, zinc oxide (ZnO) is a wide band gap semiconductor (E_g = 3.37 eV) that has a wide range of applications such as light emitting diodes, lasers, piezoelectric, chemical sensors, field emitters and solar cells[2-8]. It also exhibits high exciton binding energy, high mechanical strength, thermal and chemical stabilities, good electrochemical activities, oxidation resistivity and high chemical/photochemical stability which are rather important for various applications[1-8]. Apart from ZnO nanoparticles, ZnO nanostructures exhibit high surface-to-volume ratio, which may have potential advantages for different applications[9,10]. In recent years, there have been many reports on the preparation of ZnO nanorods by thermal evaporation, alumina templates, chemical vapor deposition and electrochemical deposition[11-14]. However, these preparation methods still involve some complex procedures, sophisticated equipment and rigorous experimental conditions. Therefore, it is necessary to develop a simple preparation route to ZnO nanorods. Herein, we demonstrate a simple, effective and economical process for synthesizing the large-scale arrays of ZnO nanorods on Zn foil at relatively low temperature of 80 °C, by a simple hydrothermal method in NaOH aqueous solution. This is a simple, large scale and low-cost method without the need for precasting ZnO nanoparticles onto the substrates as a seed layer and adding materials such as Zn^{2+} containing salts. Also, this method does not use materials that can be potential impurities (such as other anions from zinc salts). The structural and optical properties of the as-synthesized samples have been characterized and studied. Furthermore, photocatalytic activity of these ZnO films for the photocatalytic degradation of methyl orange has been investigated.

Experimental

To prepare the zinc oxide thin films, pure zinc foils with 0.15 mm (purity: 99.9% Zn) thickness were used as the substrate. Zinc oxide nanorods were grown on zinc foils as follows: the zinc foils were polished with abrasive paper and then cleaned with absolute ethanol and distilled water to remove adsorbed dust and surface contamination. Then, the zinc foil was placed in a sealed glass jar containing 80 mL aqueous solution containing 0.3 g sodium hydroxide, followed by heating the jar to the desired temperature and keeping the temperature constant until the reaction was complete. After a specified time, the zinc foil was taken out of the jar, washed several times with distilled water, and then dried in air. The as-grown product was characterized by scanning electron microscopy (Phenom ProX integrated with an EDS detector, Netherlands), and the elemental composition was estimated by energy dispersive X-ray spectroscopy. The crystalline phases were identified by XRD (Philips X´Pert). Diffraction patterns were recorded in the 2θ range from 20 to 80° at room temperature. For a crystalline semiconductor, the optical absorption near the band edge follows the Eq. (1).

$$\alpha h\upsilon = A\left(h\upsilon - E_g\right)^{n/2} \quad \text{... (1)}$$

where α, υ, E_g, and A are the absorption coefficient, light frequency, band gap energy and a constant, respectively, while n depends on the characteristics of the transition in a semiconductor, i.e., direct transition (n = 1) or indirect transition (n = 4). For ZnO, the value of n is 1 for the direct transition. The band gap energy (E_g value) of ZnO films (recorded by employing double beam UV-vis spectrophotometer, JASCO V-570) was thus estimated from a plot of $(\alpha h\upsilon)^2$ versus photon energy hυ.

The photocatalytic performance of ZnO samples for photodegradation was studied using methyl orange (MO) as a model solution. The photocatalytic reaction was carried in a single-compartment cylindrical quartz reactor, with 400 W UV lamp as a light source at room temperature. The luminous intensity of the xenon lamp was 200 mW/cm^2. The quartz glass transmitted 100% of the light as the lamp shone on the samples. The initial concentration of methyl orange was 2 mg/L. The volume of the solution was 50 mL. Prior to illumination, the photocatalyst sample was immersed in a quartz reactor containing methyl orange and magnetically stirred for 2 h in the dark to ensure the establishment of adsorption-desorption equilibrium between the photocatalyst and methyl orange. Then the solution was exposed to UV light irradiation under magnetic stirring for 2 h. At each 10 min interval, 5 mL solution was sampled and the absorbance of methyl orange was measured by a UV-vis spectrophotometer.

Results and discussion

The general morphologies of the as-prepared ZnO nanorods grown at 80 °C for 16 h were examined by scanning electron microscopy (SEM). Figure 1(a, b) shows the SEM images taken from the product on the zinc foil with different magnifications. As can be seen, the surface of the zinc foil has been coated with quasi-oriented ZnO nanorod arrays which present a diameter of about 70–90 nm and average length estimated to be in the range of 0.5–2.0 μm. Zinc oxide films grown on zinc foils were analyzed by energy-dispersive X-ray spectroscopy (EDX), which confirmed the presence of zinc and oxygen atoms, exclusively and no impurities are present in sample

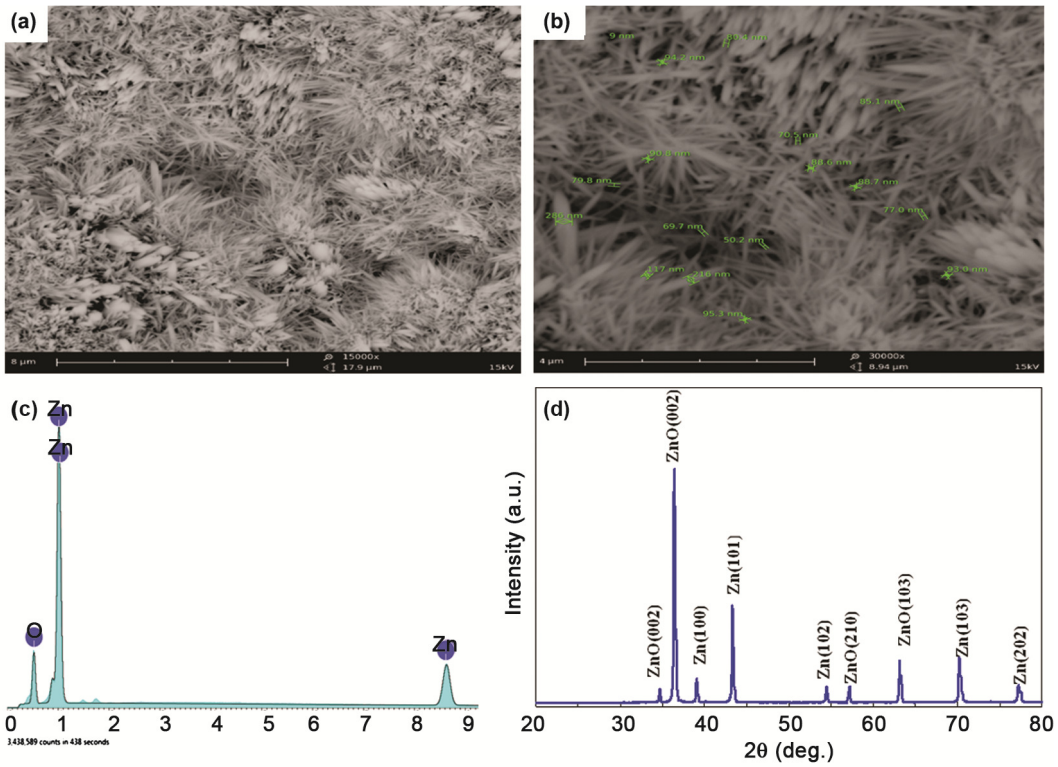

Fig. 1—(a, b) SEM top-view images of ZnO nanorod array films grown on zinc foil in the NaOH aqueous solution at 80 °C for 16 h with different magnifications [a, 15000x; b, 30000x], (c) Energy-dispersive X-ray spectroscopy analysis of ZnO films grown on zinc foil, and, (d) X-ray diffraction pattern of the as-prepared ZnO product on the zinc foil.

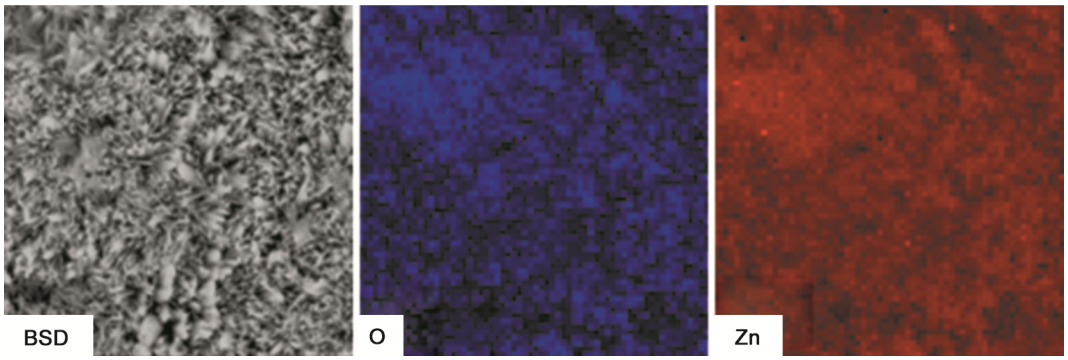

Fig. 2—Elemental mapping spectra of ZnO films containing of elements map of zinc distribution and elements map of oxygen distribution.

(Fig. 1c). The XRD patterns of ZnO nanorod can be indexed to the hexagonal wurtzite structures (hexagonal phase) (Fig. 1d). Even when it has been fabricated at low temperature, the strong and sharp diffraction peaks of ZnO indicate good crystallization of the samples. The XRD pattern shows that the peaks corresponding to the substrates have very weak intensity, indicating that the crystalline ZnO was grown densely. According to elemental mapping analysis (Fig. 2), the dispersion of zinc and oxygen is uniformly homogenous in the sample.

Diffuse reflectance spectrum of the film made of ZnO nanorod is shown in Fig. 3. The UV-vis absorption spectrum revealed that ZnO nanorod array film absorption was mainly in the UV range (below 400 nm). The plot of $(\alpha h\upsilon)^{1/2}$ versus $h\upsilon$ employed to calculate the band gap value of ZnO nanorod array thin film that provides the band gap energy as ~3.31 eV for this sample (Fig. 3). These results suggest that the films are efficient UV absorbers and moderate-weak absorbers of visible light.

To better understand the growth process of these ZnO nanostructures, the key factors influencing the process including the temperature and the reaction time were examined by SEM. Figure 4(a, b) shows the SEM images of the ZnO nanorods prepared by heating at different temperatures (50 °C and 150 °C) for 16 h. According to the SEM images, it can be concluded that at low temperature, nanostructured films were not formed on the surface (Fig. 4a). At high temperature, a porous film was formed on the surface of the Zn substrate. In addition, formation of the ZnO films at different times was analyzed. Figure 4(c, d) shows the SEM images of the ZnO films prepared at 80 °C for varying time, showing the role of the growth time on the formation and growth of the ZnO films. It is very obvious that at longer time periods, aggregation of

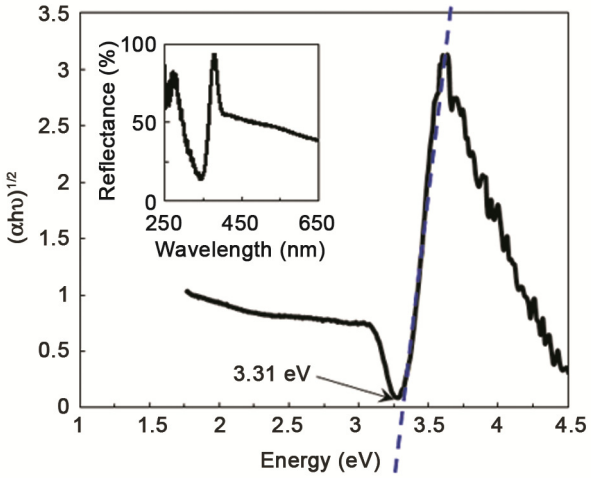

Fig. 3—Plot of $(\alpha h\upsilon)^{1/2}$ versus $h\upsilon$ employed to calculate the band gap value of ZnO nanorod array film sample. [Inset: Diffuse reflectance spectra of the ZnO nanorod array films].

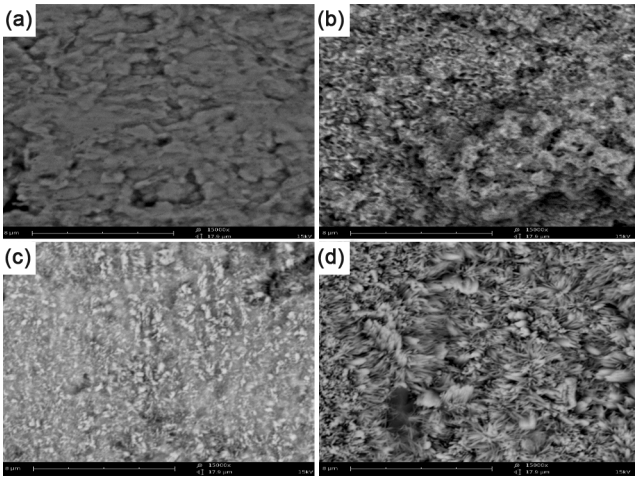

Fig. 4—(a, b) SEM top-view images of ZnO films grown on zinc foil in the NaOH aqueous solution at different temperatures for 16 h: (a) 50 °C and (b) 150 °C. (c, d) SEM images of the ZnO films prepared at 80 °C for different times: (c) 24 h and (d) 18 h.

nanorods occurred. Experiments under short time periods (less than than 16 h) were also carried out; but no ZnO nanorods were formed. These results indicate that ZnO nanorod arrays resulted when the growth time was 16 h and temperature was 80 °C.

There are several possible models for the growth of conventional 1D nanomaterials such as the helical dislocation, vapor-liquid-solid (VLS), solution-liquid-solid (SLS) and an oxide-assisted growth (OAG) mechanism[15]. Based on the SEM results, the growth process of the ZnO nanorods can be explained in terms of the solid-liquid-solid (SLS) process, which is proposed to be responsible for the 1D nanostructure growth[15-17]. According to previous research results on the formation mechanism of ZnO nanorods grown under hydrothermal conditions[18,19], the formation of the ZnO nanorods is mostly attributed to the presence of a surfactant, organic solvent or solution concentration. However, no surfactants or organic solvent was used in the present study. The starting material is only zinc substrate with water as the solvent.

It is proposed that ZnO originates from the surface of the zinc substrate owing to the oxidation and nanoclusters of Zn and ZnO nanoparticles are formed on the surface of the zinc substrate. Zn on the surface of the zinc substrate is further oxidized by the oxygen originating from the hydrothermal environment to form ZnO nanoclusters on the substrate which act as nuclei for further growth of ZnO[15]. After completion of one monolayer of ZnO nanostructure, the next layer is formed by lateral growth of new nuclei[15,20,21]. Many solid materials naturally grow in to 1D nanostructures, which are determined by highly anisotropic bonding in the crystallographic structure. As reported earlier, ZnO is a polar, hexagonal and highly anisotropic crystalline, which indicates that its oriented growth direction is along the *c*-axis[15]. The growth direction is mainly determined by the internal structure, and is also affected by external conditions, such as temperature and growth time. The growth of ZnO nanorods stops gradually due to the continuous consumption of Zn nanoparticles on the surface of the Zn substrate.

Photoluminescence (PL) spectroscopy is a very useful technique to study the efficiency of charge carrier trapping, immigration and transfer in a semiconductor[22]. Generally, the photoluminescence emissions on semiconductor materials originate from the radiative recombination of photo-generated electrons and holes; these two major photo-physical processes can give rise to photoluminescence signals.

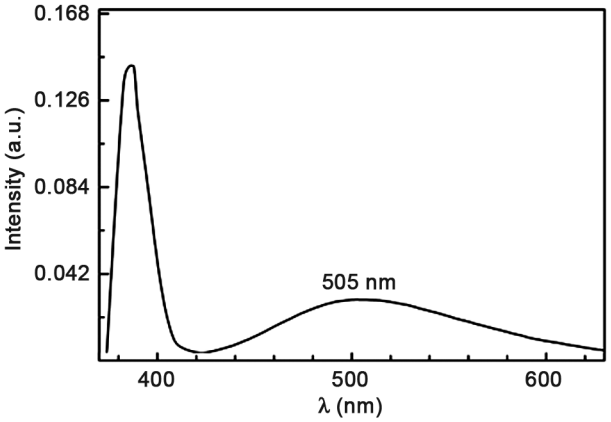

Fig. 5—Photoluminescence spectrum of the ZnO nanorods.

Figure 5 shows the PL spectrum of the ZnO nanorods for evaluating the optical properties. Two emission bands are observed; the first is a strong ultraviolet (~ 380 nm) band, and the other is a weak visible (green/yellow) emission. The UV emission located at 380 nm is assigned to the near-band-edge (NBE) emission and the visible emission located at 505 nm is related to a deep level or trap state in the ZnO nanorods, such as interstitial zinc and oxygen vacancies that act as donors at energy levels located below the conduction band edge[23]. Here, a strong UV exciton emission and weaker defect emission prove that the ZnO nanorods are of good crystal quality.

The photocatalytic activities of the synthesized ZnO samples were evaluated on the basis of the decomposition of methyl orange in aqueous solution, under exposure to UV irradiation. Methyl orange degradation experiments were conducted under UV irradiation to evaluate direct photolysis with and without the addition of any catalyst. The concentration of methyl orange remained nearly constant after 120 min of irradiation in the absence of catalyst, and no obvious degradation of methyl orange was observed in this time period. In addition, a dark control experiment was conducted, indicating that the adsorption of methyl orange onto the surface of the catalyst in the absence of light radiation was negligible. Photocatalysis studies in the presence of the catalyst indicated that the photocatalytic process was very effective in the removal of methyl orange. Figure 6 presents the rate of decomposition of the dye, where C_0 is the initial dye concentration and C_t is the concentration at a time t.

The experimental results of the photocatalytic degradation of different organic contaminants revealed that the corresponding data fit to the Langmuir-

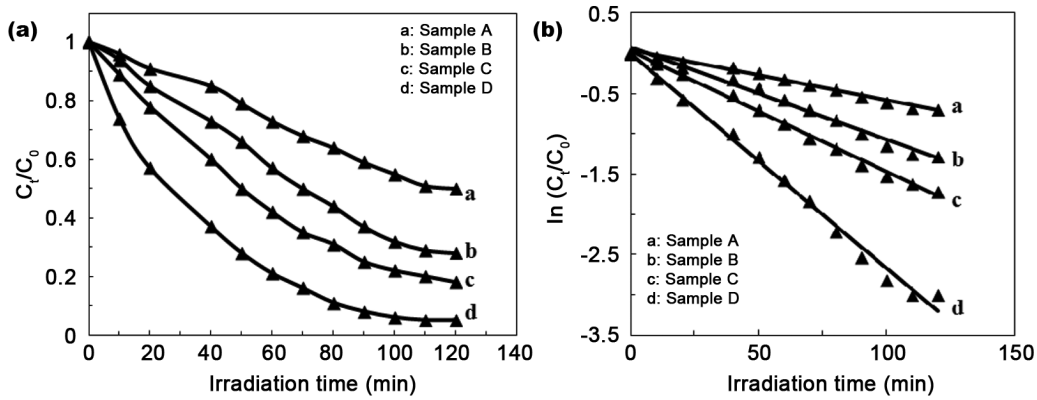

Fig. 6 (a)—Photocatalytic degradation of methyl orange (MO) over different catalyst samples (as given in Table 1) under UV irradiation, and, (b) $\ln(C_t/C_0)$ versus irradiation time.

Table 1—The apparent first-order rate constant (k) of photocatalytic degradation of methyl orange for different samples

Samples	Temp. (°C)	Time (h)	Apparent rate constant, k (min^{-1})	Corr. coeff. (R^2)
(A)	80	18	0.61×10^{-2}	0.989
(B)	150	18	1.15×10^{-2}	0.986
(C)	80	24	1.51×10^{-2}	0.996
(D)	80	16	2.67×10^{-2}	0. 992

Hinshelwood kinetic model that can be simplified to a pseudo-first-order kinetic equation as follows for dilute solutions:

$$\ln\left(\frac{C_t}{C_0}\right) = -k_{app}\, t \qquad \ldots (2)$$

where C_t is the concentration of methyl orange at time t, C_0 is the equilibrium concentration after adsorption and k_{app} is the apparent rate constant. The linear plots of $\ln(C_t/C_0)$ versus irradiation time (Fig. 6b) give the slope of linear regression as the apparent first-order rate constant k. The apparent first-order rate constants and correlation coefficients corresponding to Fig. 6(b) are listed in Table 1.

In summary, we propose a facile hydrothermal method to grow large scale ZnO nanowires on zinc foil substrates. The morphology and structure of as-prepared ZnO products were characterized by SEM, XRD and EDX. Optical properties were investigated by UV-vis diffuse reflectance spectra. The resulting ZnO nanorod showed a diameter of about 70–90 nm with the average length estimated to be in the range of 0.5-2.0 μm. The as-grown ZnO nanowires show fairly good crystallinity. UV-vis data suggest that the films are efficient UV absorbers and moderate-weak absorbers of visible light. The photocatalytic activity exhibited by the ZnO nanowires was higher than that by the other samples. The kinetics for photodegradation was pseudo-first-order and sample D prepared by heating at 80 °C for 16 h, exhibited better photocatalytic activity than other samples. Such films may find potential application as a photocatalyst for waste water treatment. The proposed method uses very little energy and requires no complex experimental procedures or equipment and can be used as a promising, simple and fast option for large scale production of ZnO nanowires.

References

1 Jamali-Sheini F, Yousefi R, Joag D S & More M A, *Vacuum,* 101 (2014) 233.
2 Bao J, Zimmler M A, Capasso F, Wang X & Ren Z F, *Nano Lett,* 6 (2006) 1719.
3 Johnson J C, Yan H, Yang P & Saykally R J, *J Phys Chem B,* 107 (2003) 8816.
4 Zhao M H, Wang Z L & Mao S X, *Nano Lett,* 4 (2004) 587.
5 Qurashi A, Faiz M, Tabet N & Waqas Alam M, *Superlattices Microstruct,* 50 (2011) 173.
6 Jamali Sheini F, Joag D S, More M A, Singh J & Srivasatva O N, *Mater Chem Phys,* 120 (2010) 691.
7 Xu C X & Sun X W, *Appl Phys Lett,* 83 (2003) 3806.
8 Zhao Q, Xu X Y, Song X F, Zhang X Z, Yu D P, Li C P & Gou L, *Appl Phys Lett,* 88 (2006) 033102.
9 Santhaveesuk T & Choopun S, *Adv Mater Res,* 770 (2013) 185.
10 Ng T N, Chen X Q & Yeung K L, *RSC Adv,* 5 (2015) 13331.
11 Zhang J, Yu W Y & Zhang L D, *Phys Lett A,* 299 (2002) 276.
12 Lee J S, Park K S, Kang M I, Park I W, Kim S W, Cho W K, Han H S & Kim S S, *J Cryst Growth,* 254 (2003) 423.
13 Sun Y, Fuge G M & Ashfold M N R, *Chem Phys Lett,* 396 (2004) 21.
14 Wu J J & Liu S C, *Adv Mater,* 14 (2002) 215.
15 Pei L Z, Zhao H S, Tan W, Yu H Y, Chen YW, Fan C G & Zhang Q F, *Physica E,* 4 (2010) 1333.

16 Zhang J, Yang Y D, Jiang F H & Li J P, *Physica E,* 27 (2005) 302.
17 Yu D P, Xing Y J, Hang Q L, Yan H F, Xu J, Xi Z H & Feng S Q, *Physica E,* 9 (2001) 305.
18 Tang L, Bao X B, Zhou H & Yuan A H, *Physica E,* 40 (2008) 924.
19 Yadav R S & Pandey A C, *Physica E,* 40 (2008) 660.
20 Hou K, Li C, Lei W, Zhang X B, Yang X X, Qu K, Wang B P, Zhao Z W & Sun X W, *Physica E,* 41 (2009) 470.
21 Momeni M M & Mirhoseini S M, *Surf Eng,* 31 (2015) 507.
22 Cong Y, Zhang J, Chen F & Anpo M, *J Phys Chem C,* 111 (2007) 6976.
23 Huang M H, Wu Y Y, Feick H, Tran N, Weber E & Yang P D, *Adv Mater*, 13 (2001) 113.